RSC Advances



PAPER

View Article Online

View Journal | View Issue



Cite this: RSC Adv., 2019, 9, 1278

Fe₃O₄@nano-cellulose/Cu(\shortparallel): a bio-based and magnetically recoverable nano-catalyst for the synthesis of 4*H*-pyrimido[2,1-*b*]benzothiazole derivatives†

Nasrin Safajoo, a Bi Bi Fatemah Mirjalili ** and Abdolhamid Bamoniri ** b

Fe₃O₄@nano-cellulose/Cu(II) as a green bio-based magnetic catalyst was prepared through *in situ* coprecipitation of Fe²⁺ and Fe³⁺ ions in an aqueous suspension of nano-cellulose. The mentioned magnetically heterogeneous catalyst was characterized by FT-IR, XRD, VSM, FESEM, TEM, XRF, EDS and TGA. In this research, the synthesis of 4H-pyrimido[2,1-b]benzothiazole derivatives was developed *via* a three component reaction of aromatic aldehyde, 2-aminobenzothiazole and ethyl acetoacetate using Fe₃O₄@nano-cellulose/Cu(II) under solvent-free condition at 80 °C. Some advantages of this protocol are good yields, environmentally benign, easy work-up and moderate reusability of the catalyst. The product structures were confirmed by FT-IR, 1 H NMR, and 13 C NMR spectra.

Received 7th November 2018 Accepted 13th December 2018

DOI: 10.1039/c8ra09203f

rsc.li/rsc-advances

Introduction

Fused heterocyclic compounds containing nitrogen and sulfur are important compounds because of their pharmacological properties.1 Among these compounds benzothiazoles and pyrimido[2,1-*b*]benzothiazoles have attracted considerable interest. Some of these compounds have various biological activities such as antiviral,2,3 antitumor,4-6 antiinflammatory,7,8 antimicrobial,10,11 antiallergic,9 anticonvulsant,12 proliferative¹³ and antifungal activities.¹⁴ Pyrimido[2,1-b]benzothiazole derivatives were synthesized through multicomponent reaction between 2-amino benzothiazole, aromatic aldehydes and β -ketoesters. Previously, this protocol has been catalyzed by iron fluoride, 19 pyridine, 11 acetic 1,1,3,3-N,N,N',N'-tetramethylguanidinium acid,20 fluoroacetate (TMGT),16 tetrabutylammonium hydrogen sulfate (TBAHS),17 N-sulfonic acid modified poly(styrene-maleic anhydride) (SMI-SO₃H),21 chitosan,18 aluminum trichloride22 and Fe₃O₄@nano-cellulose/TiCl.²³ Some of the reported protocols have harsh conditions and long reaction times. Thus, in this work, a new simple protocol for the synthesis of these compounds is reported.

Biopolymers, especially cellulose and its derivatives, have some unparalleled properties, which make them attractive alternatives for ordinary organic or inorganic supports for catalytic applications.24 Cellulose is the most abundant natural material in the world and it can play an important role as a biocompatible, renewable resource and biodegradable polymer containing OH groups.25 Cotton is a natural, cheap, and readily available source of cellulose. Fe₃O₄ nanoparticles are coated with various materials such as surfactants,26 polymers,27,28 silica,29 cellulose23 and carbon30 to form core-shell structures. Magnetic nanoparticles as heterogeneous supports have many advantages such as high dispersion in reaction media and easy recovery by an external magnet.31-38 Cu(II) as a safe and ecofriendly cation is a good Lewis acid and can activate the carbonyl group for nucleophilic addition reactions. Thus, the main purpose of the present work is the preparation of Fe₃O₄@nano-cellulose/Cu(II) as a new and bio-based magnetic nanocatalyst for one-pot synthesis of pyrimido[2,1-b] benzothiazoles via condensation of aromatic aldehydes, ethyl acetoacetate and 2-aminobenzothiazole.

Results and discussion

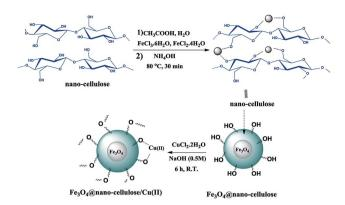
Fe₃O₄@nano-cellulose/Cu(π) was prepared in a two-step process. First, Fe₃O₄@nano-cellulose was synthesized by coprecipitation of Fe²⁺ and Fe³⁺ ions in the presence of nanocellulose and then it was used as a magnetic support for loading CuCl₂ onto the cellulose section of it (Scheme 1). The magnetically heterogeneous catalyst named Fe₃O₄@nanocellulose/Cu(π), is characterized by Fourier transform infrared (FT-IR) spectroscopy, X-ray diffraction (XRD), vibrating sample magnetometer (VSM), field emission scanning electron microscopy (FESEM), transmission electron microscopy (TEM),

[&]quot;Department of Chemistry, College of Science, Yazd University, Yazd, P. O. Box 89195-741, Islamic Republic of Iran. E-mail: fmirjalili@yazd.ac.ir; Fax: +98 3538210644; Tel: +98 3531232672

^bDepartment of Organic Chemistry, Faculty of Chemistry, University of Kashan, Kashan, Islamic Republic of Iran

[†] Electronic supplementary information (ESI) available. See DOI: 10.1039/c8ra09203f

Paper



Scheme 1 Synthesis protocol for Fe₃O₄@nano-cellulose/Cu(II).

X-ray fluorescence (XRF), energy-dispersive X-ray spectroscopy (EDS), and thermo-gravimetric analysis (TGA).

The FT-IR spectra of nano-cellulose, Fe₃O₄@nano-cellulose and Fe₃O₄(a)nano-cellulose/Cu(II) are shown in Fig. 1.

The FT-IR spectrum of nano-cellulose has shown a broad band at 3338 cm⁻¹ which corresponds to the stretching vibrations of OH groups. The absorption bands at 1058 and 1108 cm⁻¹ display the stretching vibrations of the C-O bonds. For Fe₃O₄@nano-cellulose, in addition to the cellulose absorptions bands, stretching vibrations of Fe/O groups at 586 and 634 cm⁻¹ are appeared which is indicated that the magnetic Fe₃O₄ nano particles are coated by nano-cellulose. The FT-IR spectrum of Fe₃O₄@nano-cellulose/Cu(II) has shown a characteristic absorption band under 500 cm⁻¹ that may be attributed to Cu-O band for Cu bonded to cellulose. X-ray diffraction (XRD) pattern of Fe₃O₄@nano-cellulose/Cu(II) is shown in Fig. 2. Fe_3O_4 has shown diffraction peaks at $2\theta = 35.79^{\circ}$, 43.42° , 53.94°, 57.51° and 63.08° with FWHM equal to 0.39, 0.78, 0.94, 0.31 and 0.96 respectively, which are quite matched with the cubic spinel structure of pure Fe₃O₄. A diffraction peaks at $2\theta =$ 16.45° and 22.18° with FWHM equal to 0.23 and 0.47, respectively, has shown the existence of cellulose. Other signals in 2θ = 13.68, 29.10, 32.01, 34.25 and 45.71 probably reveal the existence of cellulose and bonding of Cu(II) to cellulosic shell (Table 1).

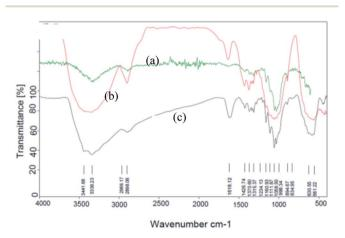
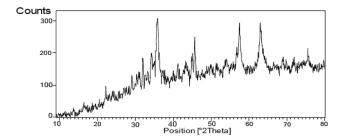


Fig. 1 FT-IR spectra of (a) nano-cellulose, (b) Fe₃O₄ @ nano-cellulose and (c) Fe₃O₄@nano-cellulose/Cu(II).



XRD pattern of Fe₃O₄@nano-cellulose/Cu(II)

The magnetic properties of Fe₃O₄ and Fe₃O₄@nano-cellulose/Cu(II) were characterized at RT (300 K) by a vibrating sample magnetometer (VSM) and their hysteresis curves are presented in Fig. 3. The zero coercivity and remanence of the hysteresis loops of these magnetic nanoparticles confirm superparamagnetic property of them at room temperature. The amount of specific saturation magnetization (Ms) for Fe₃O₄ nanoparticles was about 50 emu g⁻¹, which decreased to 25 emu g^{-1} after the bonding of Cu(II) on the surface of Fe_3O_4 nano-cellulose. Despite this significant decrease, the saturated magnetization of these magnetic nanoparticles is sufficient for magnetic separation.

The particles size of Fe₃O₄@nano-cellulose/Cu(II) were investigated by field emission scanning electron microscopy (FESEM) and transmission electron microscopy (TEM) in which the dimensions of them were achieved below 70 nm (Fig. 4). The chemical composition of catalyst has been measured using X-

Table 1 Results of XRD analysis of Fe ₃ O ₄ @nano cellulose/Cu(II)								
No.	1	2	3	4	5	6		
Pos. $[^{\circ}2\theta]$ FWHM $[^{\circ}2\theta]$	13.6815 0.6298	16.4566 0.4723	22.1853 0.2362	29.1068 0.2362	32.0094 0.3149	34.2572 0.3149		
No.	7	8	9	10	11	12		
Pos. $[^{\circ}2\theta]$ FWHM $[^{\circ}2\theta]$	35.7935 0.3936	43.4246 0.7872	45.7114 0.3149	53.9425 0.9446	57.5101 0.3149	63.0810 0.9600		

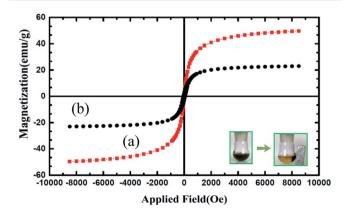


Fig. 3 Magnetization loop of (a) Fe₃O₄ and (b) Fe₃O₄@nano-cellulose/ Cu(II).

RSC Advances Paper

ray fluorescence (XRF) analysis (Table 2). In order to obtain the Cu: Cl ratio in Fe₃O₄@nano-cellulose/Cu(II) by XRF analysis, Kilo Counts Per Seconds (KCPS) values of elements in catalyst were compared with KCPS values of the same elements in pure samples, NaCl and CuSO₄. By this comparison, the amount of Cu and Cl were obtained 1.38 g (0.02 mol) and 0.12 g (0.003 mol), respectively. Thus, the ratio of Cu: Cl in catalyst is approximately 6:1.

And so, existence of Cu and Cl in catalyst was confirmed by EDS analysis data (Fig. 5).

The thermal stability of Fe₃O₄@nano-cellulose/Cu(II) was investigated by thermo-gravimetric analysis (TGA) in the temperature range of 30-800 °C (Fig. 6).

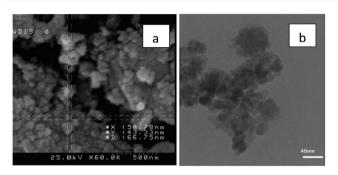


Fig. 4 (a) FESEM image of Fe₃O₄@nano-cellulose/Cu(II) and (b) TEM of Fe_3O_4 @nano-cellulose/Cu(II).

Table 2 Results of XRF analysis of catalyst, pure NaCl and CuSO₄

	Fe ₃ O ₄ @nano- cellulose/Cu(II)		CuSO ₄		NaCl	
Elemental component	KCPS	wt%	KCPS	wt%	KCPS	wt%
CO_2	1.5	74.8	0.2	13.3		
Fe_2O_3	1118.9	21.7	0.6	0.0174		
CuO	19.5	1.45	563.9	41.2		
SiO_2	2.8	0.796	0.1	0.0403		
Na_2O	0.9	0.573	0.2	0.218		
CaO	4.3	0.190	0.2	0.00479		
I	2.0	0.0799	1.2	0.145		
Cl	1.0	0.0681			516.5	62
Sb_2O_3	1.7	0.0606	0.7	0.0746		
Al_2O_3	0.2	0.0565				
SO_3	0.4	0.0523	184.8	43.7		
MnO	2.2	0.0482				
MgO	0.2	0.0432	2.2	1.02		
SnO_2	1.2	0.0340	0.7	0.0546		
Re	0.7	0.0333	0.5	0.0585		
CoO	2.2	0.0285				
Cr_2O_3	0.4	0.0100				
Pd	0.1	0.00860				
TiO_2	0.3	0.00860				
Rh	0.1	0.00747				
K_2O	0.2	0.00734				
SrO	0.5	0.00340				
Ho_2O_3			0.4	0.0446		
HfO_2			1.8	0.0381		
P_2O_5			0.1	0.0346		
Rh			0.1	0.0213		
Total		100		100		

The TGA curve illustrates four mass-loss steps. Firstly, a very small weight loss (2.53%) from 50 to 100 °C is corresponded to remove of catalyst moisture. Subsequently, the main weight loss step in the temperature ranges 200-370 °C (33%) is attributed to the decomposition of cellulose units through the formation of levoglucosan and other volatile compounds. Finally, there are two weight loss steps in the temperature ranges 400-600 and 650-690 °C (5 and 16%, respectively). According to the TG-DTA diagram of Fe₃O₄@nano-cellulose/Cu(II), it was revealed that this catalyst is suitable for the promotion of organic reactions below 200 °C.

Catalyst efficiency for synthesis of 4H-pyrimido[2,1-b] benzothiazole derivatives

After characterization of Fe₃O₄(a)nano-cellulose/Cu(II), the activity of catalyst was evaluated for the synthesis of 4H-pyrimido[2,1-b]benzothiazole derivatives.

For optimization of the reaction conditions, the reaction of 2aminobenzothiazole, 4-nitrobenzaldehyde and ethyl acetoacetate as a model reaction was investigated (Table 3). As shown in Table 3, entry 14, it was found that 0.03 g of Fe₃O₄@nano-cellulose/Cu(II) under solvent-free condition at 80 °C is the best reaction condition. In order to compare the efficiency of present nano-catalyst with other catalysts, the model reaction was also performed using the reported catalysts for the synthesis of 4H-pyrimido[2,1-b]benzothiazole derivatives. As Table 4 indicates, in comparison with other reported catalysts, we have found that Fe₃O₄@nano-cellulose/Cu(II)

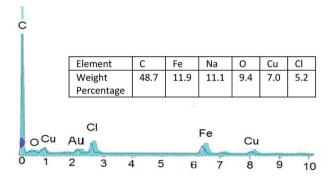


Fig. 5 EDS (EDX) spectra of Fe₃O₄@nano-cellulose/Cu(II)

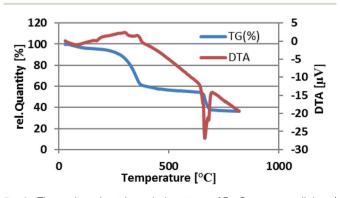


Fig. 6 Thermal gravimetric analysis pattern of Fe₃O₄@nano-cellulose/ Cu(II).

Table 3 The reaction of 2-aminobenzothiazole, 4-nitrobenzaldehyde, and ethyl acetoacetate in the presence of Fe_3O_4 @nano-cellulose/Cu(II) under various conditions⁴

Entry	Solvent	Catalyst (g)	Condition	Time (h)	Yield ^b (%)
1	_	_	80 °C	7 h	30
2	_	CuCl_2	80 °C	3h	69
3	_	Fe_3O_4	70 °C	3h	37
4	_	Fe ₃ O ₄ @nano-cellulose	80 °C	4 h	41
5	C_2H_5OH	_	R. T	7 h	_
6	C_2H_5OH	Catalyst (0.04) ^c	R. T	3 h	35
7	C_2H_5OH	Catalyst $(0.04)^c$	Reflux	3 h	57
8	H_2O	Catalyst $(0.04)^c$	Reflux	3 h	42
9	CH_3OH	Catalyst $(0.04)^c$	Reflux	3 h	51
10	_	Catalyst $(0.04)^c$	R. T	3 h	43
11	_	Catalyst $(0.04)^c$	70 °C	1 h	85
12	_	Catalyst $(0.05)^c$	80 °C	0.5	93
13	_	Catalyst $(0.04)^c$	80 °C	0.5	97
14	_	Catalyst $(0.03)^c$	80 °C	0.5	97
15	_	Catalyst $(0.02)^c$	80 °C	0.5	84
16	_	Catalyst (0.03), 2 th run ^c	80 °C	0.5	93
17	_	Catalyst (0.03), 3 rd run ^c	80 °C	0.5	88
18	_	Catalyst (0.03), 4 th run ^c	80 °C	0.5	83

^a The amount ratio of 2-aminobenzothiazole (mmol), 4-nitrobenzaldehyde (mmol) and ethyl acetoacetate (mmol) are equal to 1:1:1. ^b Isolated yield. ^c Fe₃O₄@ nano-cellulose/Cu(II).

promoted reaction has shorter reaction time, higher yields of products, green reaction conditions and simpler workup. Finally, the above optimized reaction conditions were explored for the synthesis of 4H-pyrimido[2,1-b]benzothiazole derivatives and the results are summarized in Table 5. The reusability of the catalyst was also investigated on the model reaction. The magnetic nature of the catalyst allowed its facile recovery by simple separation by an external magnet, washing with ethanol and drying at room temperature to provide an opportunity for recycling experiments. The separated nano-catalyst was reused in the above-mentioned reaction for the synthesis of IV_b for four times without considerable loss of its catalytic activity (Table 3). Partial loss of activity may be due to blockage of catalyst active sites and/or partial leaching of Cu from the catalyst.

Substituents on the aldehyde showed a significant effect in terms of the yield and reaction time under the optimized reaction conditions. The electron-withdrawing groups increase rate and yields of reaction compared to electron-donating groups. Suggested mechanism for the synthesis of 4*H*-pyrimido[2,1-*b*]benzothiazole (IV) in presence of Fe₃O₄(a) nanocellulose/Cu(II) was shown in Scheme 2. Cu(II) activate the carbonyl group of benzaldehyde (II) for Knoevenagel reaction with β -ketoesters (III) to production of intermediate (I). Meanwhile, Cu(II) activate the carbonyl group in intermediate (I) for Michael addition with 2-aminobenzothiazole and then interamolecular cyclization to production of product (IV).

The structures of the products IV_{a-m} were studied by their melting point, IR and ¹H NMR spectra. In the FTIR spectra of

Table 4 Comparative study of the present method and some other reported methods for synthesis of 4H-pyrimido[2,1-b]benzothiazole derivatives

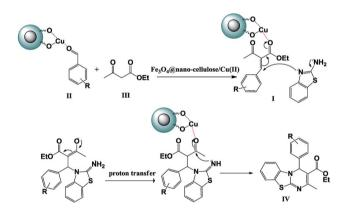
Ent.	Solvent	Catal.	Tem. (°C)	Time (h)	Yield ^a (%)	Ref.
1	CH₃OH	Acetic acid (20 mol%)	65	18	62	20
2	EG	TBAHS (30 mol%) ^b	120	2	72	17
3	HOAc	Chitosan (0.080 g)	70	1.6	93	18
4	_	TMGT $(0.080 \text{ g})^c$	100	5	53	16
5	_	AlCl ₃ (10 mol%)	65	1.2	97	22
6	_	Fe ₃ O ₄ @NCs/TiCl (0.03 g)	70	0.6	96	23
7	_	Fe ₃ O ₄ @ nano-cellulose/Cu(II) (0.03 g)	80	0.5	97	This work

^a Isolated yield. ^b Tetrabutylammonium hydrogen sulfate. ^c 1,1,3,3-N,N,N',N'-Tetramethylguanidinium trifluoroacetate.

Table 5 Synthesis of 4H-pyrimido[2,1-b]benzothiazole derivatives (IV_{a-m}) in the presence of Fe₃O₄@ nano-cellulose/Cu(II) under solvent-free condition at 80 °C a appear here with headings as appropriate

Ent.		Prod.	Time (min)	$Yield^{b}$ (%)	M. P.		
	R				Found	Report	Ref.
1	H-	IV_a	45	84	178-180	177–179	17
2	$4-NO_2-$	IV_b	30	97	171-173	170-172	22
3	4-Cl-	IV_c	30	95	87-89	86-88	21
4	4-Br-	IV_d	30	97	110-114	110-114	16
5	4-OH-	IV_e	60	82	210-212	210-212	22
6	2-NO ₂ -	IV_f	45	88	122-125	122-125	23
7	2-Cl-	$IV_{ m g}$	40	87	124-126	125-127	17
8	2-EtO-	IV_h	60	75	171-175	171-175	23
9	3-NO ₂ -	ΙV _i	35	93	222-224	222-224	21
10	3-OH-	IV _i	65	79	260-263	260-263	23
11	2,4-(Cl) ₂ -	IV_k	45	85	133-135	133-135	17
12	2,4-(MeO) ₂ -	IV_1	75	74	164-166	164-166	23
13	3,4-(OH) ₂ -	IV_{m}	70	71	225-227	225-227	23

^a I (mmol): II (mmol): Fe₃O₄(a) nano-cellulose/Cu(II) (g) is equal to 1:1:1:0.03. ^b Isolated yield.



Scheme 2 Proposed mechanism for the synthesis of 4H-pyrimido [2,1-b] benzothiazole derivatives IV_{a-m} .

products, the ester C=O stretching vibration band is appeared at 1690 cm⁻¹ due to conjugation.

Conclusions

We have demonstrated the preparation and characterization of ${\rm Fe_3O_4}$ anano-cellulose/Cu(II) as a novel magnetite recoverable, eco-friendly, inexpensive and efficient nanocatalyst. The catalytic activity of the prepared catalyst was investigated in the synthesis of 4*H*-pyrimido[2,1-*b*] benzothiazole derivatives through one-pot three-component reaction of aldehydes, ethyl acetoacetate, and 2-aminobenzothiazole under solvent-free condition at 80 °C. This protocol includes some important advantages such as mild reaction conditions, short reaction time, excellent yields, easy work-up, high purity of products.

And so, magnetic separation and reusability of nanocatalyst is other advantages of this protocol.

Experimental

General remarks

All compounds were purchased from Aldrich, Merck, and Fluka chemical companies. Nano-cellulose and Fe₃O₄@nanocellulose were synthesized via our previously reported methods.23 FT-IR spectra were run on a Bruker, Equinox 55 spectrometer. A Bruker (DRX-400 Avance) NMR was used to record the ¹H NMR and ¹³C NMR spectra. The X-ray diffraction (XRD) pattern was obtained by a Philips Xpert MPD diffractometer equipped with a Cu K α anode ($k=1.54~{
m A}^{\circ}$) in the 2θ range from 10 to 80°. XRF analysis was done with Bruker, S4 Explorer instrument. VSM measurements were performed by using a vibrating sample magnetometer (Meghnatis Daghigh Kavir Co. Kashan, Iran). Melting points were determined by a Buchi melting point B-540 B.V.CHI apparatus. Field emission scanning electron microscopy (FESEM) image was obtained on a Mira 3-XMU. Transmission electron microscopy (TEM) image was obtained using a Philips CM120 with a LaB6 cathode and accelerating voltage of 120 kV. energy-dispersive X-ray spectroscopy (EDS) of Fe₃O₄@nano-cellulose/Cu(II) was measured by an EDS instrument and Phenom pro X. Thermal gravimetric analysis (TGA) was conducted using "STA 504" instrument.

Preparation of Fe₃O₄@nano-cellulose/Cu(II)

In a flask containing 50 ml of 0.5 M NaOH, Fe $_3$ O $_4$ @nanocellulose (0.5 g) was added with stirring. Then, 75 ml of CuCl $_2$

Paper **RSC Advances**

aqueous solution, 0.04 M, was added. A dark blue solution was obtained immediately that was stirred at room temperature. After 6 h, the magnetically heterogeneous catalyst, Fe₃O₄@nano-cellulose/Cu(II), removed from solution by an external magnet. The catalyst washed with ethanol and water two times and dried at an oven at 80 °C.

General procedure for synthesis of 4H-pyrimido[2,1-b] benzothiazole derivatives

A mixture of 2-aminobenzothiazole (1 mmol), aldehyde (1 mmol), ethyl acetoacetate (1 mmol) and Fe₃O₄@nano-cellulose/ Cu(II) (0.03 g) was heated at 80 °C. After completion of the reaction (monitored by TLC), the reaction mixture was dissolved in hot ethanol (3 ml) and the catalyst was separated by using an external magnet. Subsequently by adding water to the decanted solution, the product was appeared as a pure solid in high yields. The recovered catalyst was washed 3 times with ethanol, dried and reused for subsequent runs under the same reaction conditions.

Conflicts of interest

There are no conflicts to declare.

Acknowledgements

The Research Council of Yazd University is gratefully acknowledged for the financial support for this work.

Notes and references

- 1 G. P. Ellis, Chemistry of heterocyclic compounds: synthesis of fused heterocycles, Wiley, New York, vol. 47, 2009.
- 2 A. D. Borthwick, D. E. Davies, P. F. Ertl, A. M. Exall, T. M. Haley, G. J. Hart, D. L. Jackson, N. R. Parry, A. Patikis, N. Trivedi, G. G. Weingarten and J. M. Woolven, J. Med. Chem., 2003, 46, 4428-4449.
- 3 M. A. El-Sherbeny, Arzneim.-Forsch./Drug Res., 2000, 50, 848-853.
- 4 A. M. Youssef and E. Noaman, Arzneim.-Forsch./Drug Res., 2007, 57, 547-553.
- 5 A. Y. Hassan, Phosphorus, Sulfur Silicon Relat. Elem., 2009, 184, 2856-2869.
- 6 M. T. Gabr, N. S. El-Gohary, E. R. El-Bendary and M. M. El-Kerdawy, Eur. J. Med. Chem., 2014, 85, 576-592.
- 7 V. K. Deshmukh, P. Raviprasad, P. A. Kulkarni and S. V. Kuberkar, Int. J. Chem. Tech. Res., 2011, 3, 136-142.
- 8 D. V. Kashinath, Y. M. Rajmani and C. S. Ravindra, J. Pharm. Res., 2013, 6, 574-578.
- 9 A. Bartovič, D. Ilavský, O. Šimo, L. Zalibera, A. Belicová and M. Seman, Collect. Czech. Chem. Commun., 1995, 60, 583-593.
- 10 K. R. Lanjewar, A. M. Rahatgaonkar, M. S. Chorghade and B. D. Saraf, Indian. J. Chem., Sec. B, 2009, 48, 1732-1737.
- 11 P. K. Sahu, P. K. Sahu, S. K. Gupta, D. Thavaselvamd and D. D. Agarwal, Eur. J. Med. Chem., 2012, 54, 366-378.

- 12 M. M. M. Gineinah, Sci. Pharm., 2001, 69, 53-61.
- 13 I. Ćaleta, M. Grdiša, D. Mrvoš-Sermek, M. Cetina, V. Tralić-Kulenović, K. Pavelić and G. Karminski-Zamola, Il Farmaco, 2004, 59, 297-305.
- 14 S. Maddila, S. Gorle, N. Seshadri, P. Lavanya and S. B. Jonnalagadda, Arabian J. Chem., 2016, 9, 681-687.
- 15 A. A. Pavlenko, K. S. Shikhaliev, A. Y. Potapov and D. V. Krylsky, Chem. Heterocycl. Compd., 2005, 41, 796-797.
- 16 A. Shaabani, A. Rahmati and S. Naderi, Bioorg. Med. Chem. Lett., 2005, 15, 5553-5557.
- 17 L. Nagarapu, H. K. Gaikwad, J. D. Palem, R. Venkatesh, R. Bantu and B. Sridhar, Synth. Commun., 2013, 43, 93-104.
- 18 P. K. Sahu, P. K. Sahu, S. K. Gupta and D. D. Agarwal, Ind. Eng. Chem. Res., 2014, 53, 2085-2091.
- 19 A. B. Atar, Y. S. Jeong and Y. T. Jeong, Tetrahedron, 2014, 70, 5207-5213.
- 20 P. K. Sahu, P. K. Sahu, Y. Sharma and D. D. Agarwal, J. Heterocycl. Chem., 2014, 51, 1193-1198.
- 21 M. M. Heravi, E. Hashemi, Y. S. Beheshtiha, K. Kamjou, M. Toolabi and N. Hosseintash, J. Mol. Catal. A: Chem., 2014, 392, 173-202.
- 22 P. K. Sahu, P. K. Sahu, J. Lal, D. Thavaselvam and D. D. Agarwal, Med. Chem. Res., 2012, 21, 3826-3834.
- 23 S. Azad and B. B. F. Mirjalili, RSC Adv., 2016, 6, 96928–96934.
- 24 D. Klemm, B. Heublein, H. P. Fink and A. Bohn, Angew. Chem., Int. Ed., 2005, 44, 3358-3393.
- 25 A. Shaabani and A. Maleki, Appl. Catal., A, 2007, 331, 149-151.
- 26 Y. Lu, X. Lu, B. T. Mayers, T. Herricks and Y. Xia, J. Solid State Chem., 2008, 181, 1530-1538.
- 27 H. F. Rase, Handbook of Commercial Catalysts: Heterogeneous Catalysts, CRC Press, New York, 2000.
- 28 A. El Harrak, G. Carrot, J. Oberdisse, C. Eychenne-Baron and F. Boué, Macromolecules, 2004, 37, 6376-6384.
- 29 P. Tartaj and C. J. Serna, J. Am. Chem. Soc., 2003, 125, 15754-15755.
- 30 Z. Zhang, H. Duan, S. Li and Y. Lin, Langmuir, 2010, 26, 6676-6680.
- 31 B. Rác, A. Molnar, P. Forgo, M. Mohai and I. Bertóti, J. Mol. Catal. A: Chem., 2006, 244, 46-57.
- 32 Y. Shen, J. Tang, Z. Nie, Y. Wang, Y. Ren and L. Zuo, Sep. Purif. Technol., 2009, 68, 312-319.
- 33 B. Movassagh, A. Takallou and A. Mobaraki, J. Mol. Catal. A: Chem., 2015, 401, 55-76.
- 34 T. Zeng, W. W. Chen, C. M. Cirtiu, A. Moores, G. Song and C. J. Li, Green Chem., 2010, 12, 570-573.
- 35 M. A. Zolfigol, A. R. Moosavi-Zare, P. Moosavi, V. Khakyzadeh and A. Zare, C. R. Chim., 2013, 16, 962-966.
- 36 M. A. Zolfigol, V. Khakyzadeh, A. R. Moosavi-Zare, A. Rostami, A. Zare, N. Iranpoor, M. H. Beyzavi and R. Luque, Green Chem., 2013, 15, 2132-2151.
- 37 A. Khazaei, F. Gholami, V. Khakyzadeh, A. R. Moosavi-Zare and J. Afsar, RSC Adv., 2015, 5, 14305–14310.
- 38 A. Khazaei, A. R. Moosavi-Zare, F. Gholami and V. Khakyzadeh, Appl. Organomet. Chem., 2016, 30, 691-694.